Multimode 200 GHz-spaced dense wavelength division demultiplexing for local area networks

Jie Qiao, Feng Zhao, Jizuo Zou, and Ray T. Chen
[*]Microelectronics Research Center, Department of Electrical and Computer Engineering
The University of Texas at Austin, Austin, Texas 78758

William W. Morey, James W. Horwitz, Ray Collins, George Chang, and Victor Villavicencio
Radiant Photonics Inc.
Braker "B", 1908 Krama Lane, Austin, Texas 78758

ABSTRACT

We describe the design and performance of a multimode 8-channel, 200GHz-spaced dense wavelength division demultiplexer (DWDM) using a high order blazed grating. The mean insertion loss of this DEMUX is 1.95dB. Adjacent crosstalk is measured to be better than -45dB. The temperature test cycling from 20 to 60°C indicates that the wavelength thermal drift is less than 0.00033nm/°C. The device has multi-mode fibers for both input and output, which is good for the optical networks in both metropolitan and local areas. The device is not sensitive to the disturbance of temperature and environment, so no temperature controller is needed.
Key words: Multimode dense wavelength division demultiplexer, echelle grating, dispersion ability, DWDM packaging

1. INTRODUCTION

Due to the explosive demand for high-bandwidth applications, Multimode dense wavelength division multiplexing has become an essential, robust, and high-performance data link technology in metropolitan and local area networks (MANs and LANs)[1,2]. Multimode fiber is the sizeable portion of the fibers used in LANs and air-link due to its low-cost installation, maintenance, since it was being installed in the LAN as early as the 1980's [3]. WDM has been a cost-effective method of increasing the capacity of long-haul fiber links. But the WDM for data communications has to be very low cost, compact, and compatible with multimode fiber. The potential for a large number of closely spaced channels and the inherent advantage of compactness make bulk grating based demultiplexers very attractive for multimode dense WDM applications[4,5]. Meanwhile, there is also an urgent need to find a way to overcome the temperature dependence of multimode DEMUX, and to decrease the cost and the device size. In this letter we present an athermal low loss and low crosstalk DEMUX for MANs and LANs area networks.

2. DEVICE CONFIGURATION

The device was designed to have eight channel outputs and operated in the frequency region from 192.1THz to 193.5 THz (wavelength from 1549.3 to 1560.7nm) within the ITU grid. The channel spacing is 200 GHz. Fig. 1 shows a schematic diagram of this device. The input optical signals coming from a tunable external cavity semiconductor laser passed through a mode scrambler and then 1-kilometer of coiled multimode fibers, which was used as a mode scrambler. The source was then introduced to the demultiplexer through the first channel of a silicon V-grooved multimode fiber array. This 62.5/125μm multimode fiber array has one input fiber and eight output fibers placed in a silicon V-grooves, which was designed to have non-uniform fiber spacing due to the nonlinear effect of the angular dispersion. A design optimized diffraction limited triplet lens was used to collimate the incident light from the inputs and focus the diffracted lights from the grating into the corresponding fiber array channels. A high order blazed reflection Echelle grating diffracted the incident light beams into

[*] *Email: raychen@uts.cc.utexas.edu, Phone: 512-471-7035, Fax: 512-471-8575*

WDM and Photonic Switching Devices for Network Applications II, Ray T. Chen, G. Ferris Lipscomb, Editors,
Proceedings of SPIE Vol. 4289 (2001) © 2001 SPIE · 0277-786X/01/$15.00

different angles and positions. A high-order blazed grating has several special properties, which make it an excellent wavelength dispersion component for WDM. Most apparent is its high dispersion, which permits compact optical systems with a high throughput and high resolution. In addition, because it is never used far from the blaze direction, the grating's efficiency remains relatively high over a large spectral range. Furthermore, when the grating is operated at higher orders, it is nearly free of the polarization effect. Yet another useful property comes into play under the Littow mount condition[6], which produces the same incident angle and diffraction angles. Under this condition, one lens alone can collimate and focus the light simultaneously, resulting in lower cost and decreased packaging size for the WDM system. The grating was gold coated for high reflectivity.

The multiplexer was fabricated as a stand-alone unit employing a stainless steel housing to provide compatible thermal expansion coefficient with the lens material. The entire assembling and packaging process is passive and epoxy free, which avoided the wavelength and insertion lost shifting caused by the UV curing of epoxy. By means of improving the mechanical design, the choice of the optical materials, employing the epoxy free packaging and sealed package housing, we have obtained very good thermal behavior for this DEMUX, from the point view of insertion loss, as well as the center wavelength accuracy.

3. THERMAL STABILITY ANALYSIS

When temperature changes, the insertion loss and center wavelength may change accordingly. The center wavelength shift is caused mainly by the change of groove spacing of the grating. The change of insertion loss is due to the thermal variation in lens focal length, and the image shift in lateral, and vertical direction caused by the center wavelength shift, and the difference of thermal coefficient of expansion (TCE) of lens and its supporting material respectively. We will show in this section that it is possible to eliminate or reduce the thermal effect by careful optical design, choosing the materials for making the grating, lens, and housing.

a) Central wavelength shift of individual channels: from grating equation [7]

$$\Lambda(\sin\theta_i - \sin\theta_d) = m\lambda \tag{1}$$

Where Λ is the grating groove period, θ_i, θ_d are incident and diffraction angle respectively. m is grating working order, and λ is the working wavelength.

The definition of the TCE of grating:

$$\Lambda = \Lambda_0(1 + \beta \cdot \Delta T) \tag{2}$$

Where β is the TCE of grating, ΔT is the change of temperature. Λ_0 is the groove period at temperature T_0. Λ is the groove period after temperature changes ΔT. Assuming the incident and diffraction angle keep constant with temperature, we can easily find the wavelength shift with temperature:

$$\Delta\lambda = \beta \ \ \lambda \ \ \Delta T \tag{3}$$

Equation (3) shows that the change in wavelength at any output fiber is proportional to the thermal coefficient of expansion of the grating, the original wavelength, and the change in temperature. When λ=1550nm, temperature changes from 20 to 60°C (ΔT=40°C), Δλ=0.037nm. The experiment results also confirmed that wavelength shift is less than 0.04nm when temperature changes from 20 to 60°C.

b) Insertion loss shift

The shift of insertion loss with temperature variation is mainly due to the change of lens focal length and vertical and lateral image shift. The change of lens focal length is usually within the depth of focal length, which can be ignored. The image shift in vertical direction can be expressed as:

$$\Delta x = \tfrac{1}{2} D\Delta T(\beta_L - \beta_M). \tag{4}$$

Where, D is the diameter of lens, ΔT is the change of temperature, β_L and β_M are the TCE of lens and its supporting parts. Equation (4) indicates that, when temperature changes within a certain degree, the smaller the difference of TCE of lens and its supporting materials, or the smaller the diameter of the lens, the less the image shift, and then the less insertion loss shift. In our design lateral image shift is less than 1.0μm.

$$\frac{d\theta_{diff}}{d\lambda} = \frac{2\tan\theta_{diff}}{\lambda} \tag{5}$$

Because the WDM system is symmetric in lateral direction, the image shift in lateral direction is mainly caused by the change of central wavelength.

Where θ_{diff} is the diffraction angle at a working wavelength λ. The lateral image shift Δy can be expressed as:

$$\Delta y = \frac{2 \cdot \Delta\lambda \cdot \tan\theta_{diff} \cdot f}{\lambda} \tag{6}$$

Where $\Delta\lambda$ is the shift of working wavelength caused by temperature variation. f is the focal length. Combining equation (3) and (6), We can easily obtain the relation between lateral shift and TCE of grating material and temperature change.

$$\Delta y = 2\beta \cdot \Delta T \cdot f \cdot \tan\theta_{diff} \tag{7}$$

It is obvious that the larger the diffraction angle, or the larger the TCE of grating material, the greater the lateral image shift with temperature. In our design, the lateral image shift is effectively suppressed to be less than 0.6μm. The insertion loss caused by image shift in either direction is ignorable considering the large core size of multimode fiber. The conclusion obtained in this section based on the assumption that the alignment is perfect. In the real case, any mis-alignment will affect the thermal stability accordingly.

4. SIMULATION FOR THE TOLERANCE OF IMAGE SHIFT

WDM laser sources usually contain a spectral width that depends on laser cavity structures and on operating conditions, laser wavelength shift is also present when the laser is internally modulated [8]. Disturbances caused by laser drifting, temperature change, and vibration are reflected as a relative movement of the input light spot at receiving fiber or as a shifting of wavelength, so larger one dB pass band and image shift tolerance are highly demanded in telecommunication networks. The smaller the ratio of the distance between the adjacent receiving fibers to the core diameter, the larger the 1dB passband [9]. To calculate the transverse loss of the WDM system, suppose the core diameter of the receiving fiber to be $D=2R$, and the diameter of the input light spot to be $d=2r$. We express the ratio of energy in the area of overlap (input light spot and receiving fiber) to energy in the entire area of the input light spot as:

$$\eta = \frac{\int_{s'} f'(x,y)ds'}{\int_{s} f(x,y)ds} \tag{8}$$

where η is the ratio of energy, s' is the overlap area, s is the input light spot area. $f'(x,y)$, $f(x,y)$ are the optical power distribution function at the overlap area and the whole area of input light spot respectively. Figure 2 illustrates equation (6). We can obtain the maximum tolerance of image shift of when the WDM system functions within 1-dB passband range.

Here, we assume a uniform power distribution across the whole area of the input light spot. We set up two simulations for the theoretical 1-dB passband calculation, in which $D= 2R=62.5\mu m$. $d =2r= 62.5\mu m$. Figure 3 shows the simulation result, which indicates that when a system is diffraction limited, i.e., the input spot size is the same as the multi-mode fiber core diameter, the maximum image shift tolerance can be up to ±10μm within 1dB passband. This large image shift tolerance is good for the device to resist kinds of environmental disturbances.

5. HIGH DATA TRANSMISSION BIT RATE

To achieve a high data transmitting bit rate in the telecommunication fields is the goal of the WDM technology. In the communications network, the WDM system is one part of the transmission regime. The pulse broadening of grating based

DWDM imposes inherent limitations on the data transmission bit rate. We need to optimize the WDM design to decrease pulse broadening which can be calculated by the formula below:

$$\Delta\tau = \frac{n_0 \frac{dy}{d\lambda} \cdot \lambda \cdot NA}{2 \cdot c} \tag{9}$$

Where, n_0 is the refractive index of media where light is transmitted. C is the speed of light at vacuum. NA=0.275, is the numerical aperture of input fiber. $dy/d\lambda=0.156mm/nm$, is the linear dispersion of the WDM system. Data transmission bit rate can be expressed as equation (10):

$$BR = \frac{1}{4\Delta\tau} \tag{10}$$

Equation (9) and (10) clearly show that, when working at a certain wavelength, the smaller the numerical aperture of input fiber, or the linear dispersion of the WDM system, the smaller the pulse broadening, then, the larger date rate.

Here $\Delta\tau=1.1\times10^{-10}$ s, theoretical bit rate, $BR = 2.3Gb/s$. Our experiment confirms a maximum *2.0 GBS* data transmission rate. They are in good agreement.

7. RESULTS

We measured the transmission spectrum using an ASE light source and an optical spectrum analyzer having a 0.01nm resolution. All the measurement results are obtained after taking the average of three sets of the input and output signals. Fig. 4 shows the transmission spectrum for each of the 8-channels. These figures were measured at the wavelength of minimum loss, which was always within 0.04nm of the nominal channel center wavelength. The lowest insertion loss for any channel was 1.50 dB, all of the channels show under 2.70dB loss with a mean figure of 1.95dB, which includes connector loss. Of the 1.95 dB, 1.25dB is due to the grating diffracting 75% of incident power into the desired diffraction order. 0.3dB is caused by lens transmission and reflection loss and the other 0.4dB is caused by fiber array coupling and connection loss.

We also monitored the change of insertion loss and center wavelength when increasing the operating temperature from 20°C to 60 °C. The average insertion loss changed from 1.95dB to 2.34dB, which gave us 0.00975dB/degree loss shift. Figure 5 shows the loss variation against different channels at 20°C and 60°C. We can find that the maximum change of the 8 channels in loss is 1.1dB, which is within the loss deviation range 1.2dB of different channel at room temperature. The average wavelength shift with temperature is 0.00033nm/°C.

The wavelength temperature dependence was successfully suppressed within 0.032nm in the 20 to 60°C temperature ranges, which is also within the wavelength accuracy range at room temperature. The measured detail device parameters are listed in table 1. The wavelength accuracy is within 0.04nm, the worst case, which is due to the imperfect positions of fibers in the array and the output power shifting of the white band ASE light source. The device has fairly good isolation and the average crosstalk is 46.5dB. The measured 1dB, 3dB bandwidths are 0.34, 0.60nm respectively. The typical polarization dependence loss was measured to be 0.13dB.

8. CONCLUSION

We designed and demonstrated a high resolution and low insertion loss athemal 8-channel DEMUX. This device has 1.95 and 2.34dB insertion loss at 20°C and 60°C respectively. The mean crosstalk is 46.7dB. To the authors' knowledge those are the best-reported result for multimode DWDM. The wavelength accuracy is within 0.04nm. The 3dB passband was measured to be 0.40nm. This low cost and high stable DEMUX can be employed for metropolitan and local area networks.

Reference:

[1] R.R Patel, H.E. Garrett, M.A. Emanuel, M.C. Larson, M.D. Pocha, D.M. Krol, R.J. Deri and M.E. Lowry: "WDM filter modules in compact, low-cost plastic packages for byte-wide multimode fiber ribbon cable data links", Electronics Letters May 13th 1999, Vol. 35, No.10

[2] Jie Qiao, Feng Zhao, Jian liu, Ray T. Chen , "Dispersion-enhanced Volume Hologram for Dense Wavelength-Division Demultiplexer", IEEE Photonics Technology Letters, VOL. 12, No. 8, August 2000, pp. 1070-1072
[3] R.C. Lasky, U.L. Osterberg, and D.P.Stigliani, *Optoelectronics for Data Communications*, pp.2, New York: Academic. 1995
[4] Kanabar,Y.;Baker,N.;Cannell,G.J.;Robertson,A.J. "High density wavelength division multiplexing for multiple access networks" , Optical Multiple Access Networks, IEE Colloquium on 1991, Page(s): 9/1 -9/4
[5] Jie Qiao, Feng Zhao, James W. Horwitz, Ray T. Chen, "32 Channel 100GHz-Spaced Demultiplexer for Metropolitan Area Network" Submitted to SPIE Optical Engineering
[6] J.P.Laude, *Wavelength Division Multiplexing* (Prentice Hall, 1993)
[7] R.R.A. Syms, *Practical Volume Holography*, Clarendon press (Oxford, 1990)
[8] P. Bhattacharya. *Semiconductor Optoelectronic Devices* (Prentice-Hall, New Jersey, 1994), 323.
[9] Jay Hirsh, Viken Y. Kalindjian, Freddie S. Lin, Michael R. Wang, Guoda Xu, Tomasz Jannson, "High channel density broadband wavelength division multiplexers based on periodic grating structures", SPIE Vol. 2532/171.

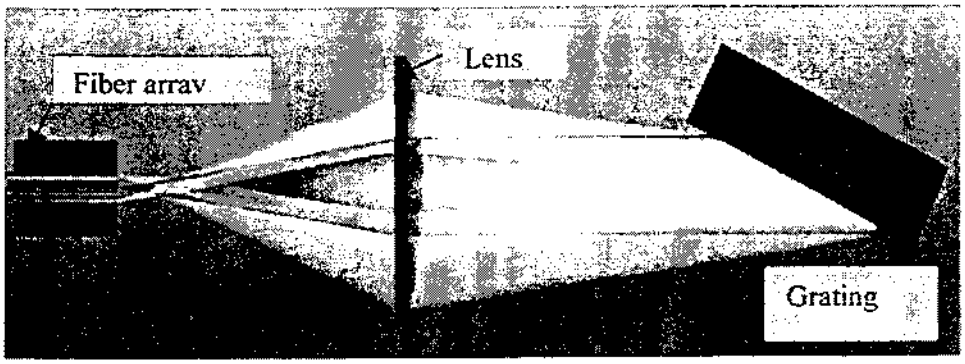

Fig.1 Geometrical layout of an eight-channel multimode demultiplexer

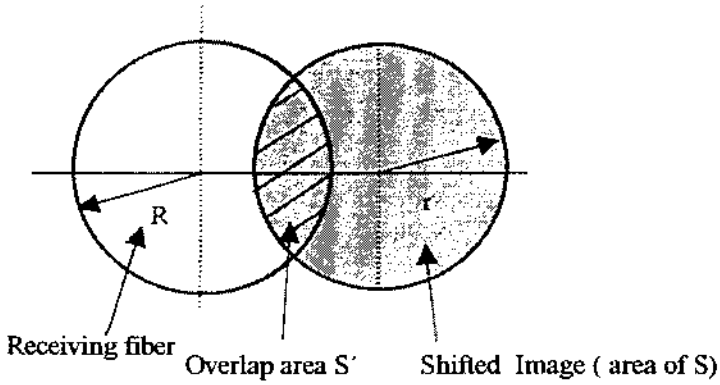

Fig. 2: Illustration of the overlap region of a receiving fiber and the input spot.

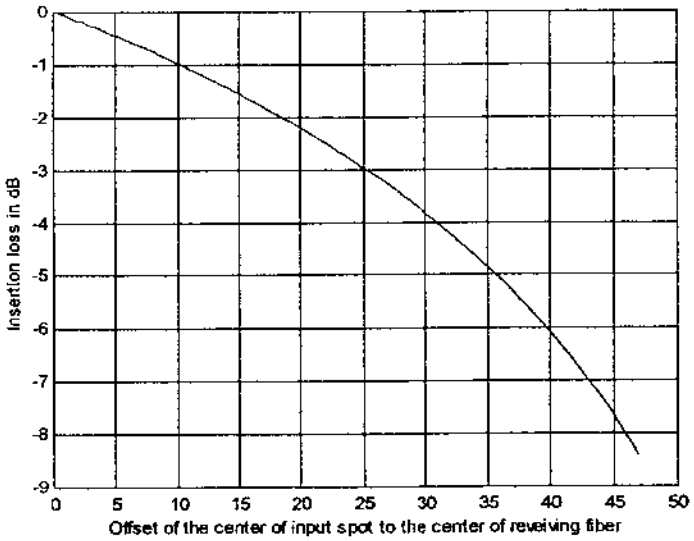

Fig. 3: Simulation result of transverse loss verse offset of a receiving fiber to the input spot.

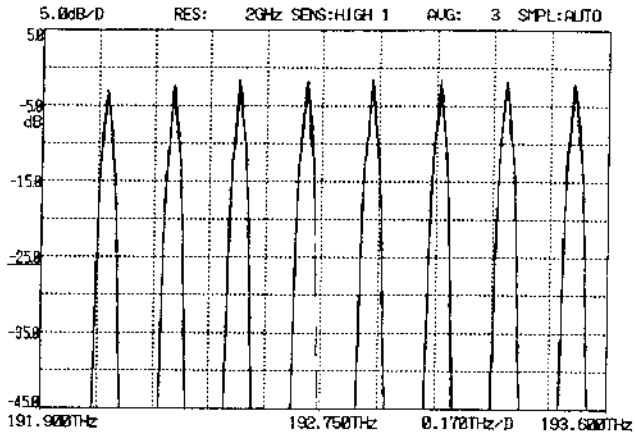

Fig.4: Output spectrum of the Demultiplexer. The resolution of the optical spectrum analyzer is 0.01nm. The measurement result is obtained by taking the average of three sets of the input and output signals.

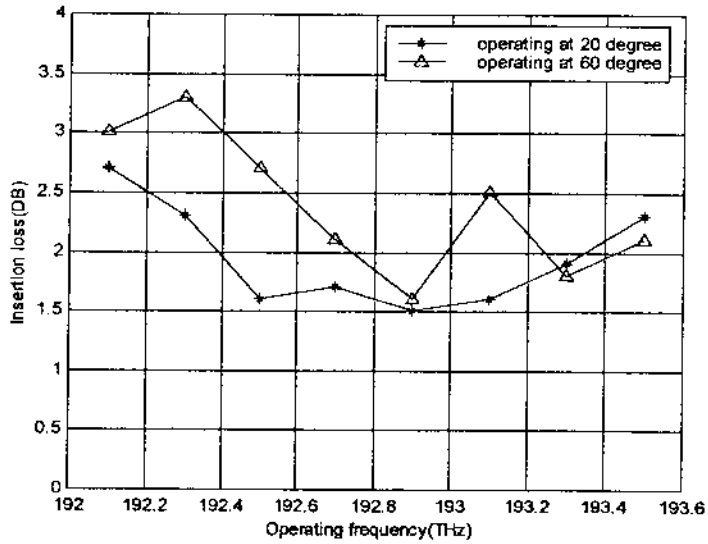

Fig. 5: Insertion loss variation plotted against channel frequency at 20°C and 60°C

Table 1: Device parameters of the multimode Demultiplexer.

	Ch#1	Ch# 2	Ch# 3	Ch# 4	Ch# 5	Ch# 6	Ch# 7	Ch#8
Designed Center wav. (nm)	1560.61	1558.98	1557.36	1555.75	1554.13	1552.52	1550.92	1549.32
Waveleng. Error at 20°C (nm)	0.02	0.02	0.04	0	0.02	0.01	0	0.02
Waveleng. Error at 60°C (nm)	0.02	0.04	0.008	0.008	0.016	0.032	0.032	0.024
Insertion loss (dB)	2.7	2.3	1.6	1.7	1.5	1.6	1.9	2.3
CrossTalk (dB)	47.8	47.6	48	48	46	45.7	44.6	44.4
3dB BW (nm)	0.60	0.61	0.60	0.60	0.60	0.62	0.60	0.60
PDL(dB)	0.2	0.15	0.07	0.1	0.28	0	0.16	0.07